Reference: *Biol. Bull.* **227:** 7–18. (August 2014)

Formation of the Statolith in the Ctenophore *Mnemiopsis leidyi*

SIDNEY L. TAMM*

Bell Center, Marine Biological Laboratory, Woods Hole, Massachusetts 02543

Abstract. The aboral sensory organ (apical organ) of ctenophores contains a statocyst with a single large statolith. The statolith comprises living cells (lithocytes), each containing a large membrane-bound concretion. The statolith is supported on the distal ends of four compound motile mechanoresponsive cilia (balancers) which control the beat frequencies of the eight locomotory comb rows, and thereby the orientation of animals to gravity. In *Mnemiopsis leidyi* and *Pleurobrachia pileus,* lithocytes arise in the thickened epithelial floor of the apical organ on opposite sides along the tentacular plane. Lithocytes progressively differentiate and migrate toward the apical surface where they bud off next to the bases of the balancers. New lithocytes are transported up the balancers by ciliary surface motility to form the statolith (Noda, 2013). The statolith has a super-ellipsoidal shape due to the rectangular arrangement of the four balancers and the addition of new lithocytes to its ends *via* the balancers. The size of the statolith increases with animal size, starting at the highest rate of growth in younger stages and gradually decreasing in larger animals. The total number of developing lithocytes in the epithelial floor increases rapidly in smaller animals and reaches a plateau range in larger animals. Lithocytes are therefore produced continually throughout life for enlargement of the statolith and possibly for turnover and replacement of existing lithocytes. The dome cilia enclosing the statocyst were observed to propagate slow, low-ampitude waves distally. The dome cilia may act as an undulating screen to prevent foreign objects in the seawater from being transported non-specifically up the balancers to make a defective statolith.

Introduction

Organisms capable of locomotion have equilibrium receptor systems that use the gravitational field as a reference (Horridge, 1969, 1971; Budelmann, 1988). Gravity receptors, known as statocysts in aquatic invertebrates, are considered to have evolved from underwater vibration receptors (Horridge, 1969, 1971) and to be the earliest true sense organs (Bullock and Horridge, 1965). The structural and functional diversity of statocysts in various invertebrates is well known (Horridge, 1969, 1971; Budelmann, 1988). A common feature is a fluid-filled cavity that contains a mass (a single statolith or numerous statoconia) of higher specific weight than the surrounding fluid that can load and mechanically stimulate underlying sensory elements, resulting in behavioral responses to gravity (Horridge, 1969, 1971; Budelmann, 1988). In vertebrates, this organ is called an otocyst with an otolith or otoconia (Budelmann, 1988).

Ctenophores, or comb jellies, are a distinct phylum of gelatinous marine zooplankton with eight meridional rows of ciliary comb plates used for locomotion (Horridge, 1965; Tamm, 1982, 2014a, b; Hernandez-Nicaise, 1991; Pang and Martindale, 2008). Phylogenetic analysis indicates that ctenophores are the sister lineage to all other animals (Ryan *et al.,* 2013). The patterns of normally developing comb rows in larval and adult ctenophores have recently been compared to the regeneration of comb plates after their surgical removal, advancing our understanding of both processes in ctenophores (Tamm, 2012a, b).

The ctenophore statocyst exploits both motile and sensory functions of cilia (Tamm, 1982, 2014a, b). The single large statolith consists of an aggregate of numerous living cells (lithocytes), each filled with a large membrane-bound calcareous concretion surrounded by a thin peripheral zone of cytoplasm and the nucleus (Samassa, 1892; Krisch, 1973; Aronova, 1974; Tamm, 1982, 2014a). The statolith is firmly held upon the tips of four sickle-shaped balancers, each located in one of the body quadrants, and each comprising 150–200 motile mechanoresponsive cilia. The balancers are linked to narrow tracts of short cilia (ciliated grooves)

Received 2 April 2014; accepted 20 June 2014.
* To whom correspondence should be addressed. E-mail: tamm@bu.edu

which run to the comb rows and act as pacemakers to mechanically stimulate beating of different comb rows (Horridge, 1965; Tamm 1982, 2014a, b). The beat frequency of the balancers depends upon the amount by which they are bent under the gravitational load of the statolith and the direction of bending (Tamm, 1982, 2014a, b). The balancer cilia serve as both mechanoreceptors and direct effectors for controlling swimming direction and orientation of ctenophores with respect to gravity (Horridge, 1965; Tamm, 1982, 2014a, b). Unlike other invertebrate statocysts, the ctenophore statocyst does not require neural or muscular responses to mediate geotaxis (Tamm, 1982, 2014a, b).

It has long been known that lithocytes arise from the thickened epithelial floor of the statocyst in ctenophores (Chun, 1880; Samassa, 1892; Tamm, 1982). The mystery of how lithocytes come to be stuck together into a statolith at the tops of the balancers has recently been solved by the discovery that newly budded lithocytes are transported up the balancers by ciliary surface motility to build the statolith (Noda, 2013).

This paper describes the spatial and temporal development of lithocytes, and how their novel delivery route into the statolith and the rectangular arrangement of their ciliary scaffold results in a superellipsoidal shape and a specific orientation of the statolith.

Materials and Methods

Organisms

Mnemiopsis leidyi Agassiz, 1865, was the main species used; individuals were dipped from the sea with a beaker attached to a pole at Woods Hole, Massachusetts. *Pleurobrachia pileus* (Müller, 1776) was also collected after work on *Mnemiopsis* was largely completed. Freshly caught animals were used immediately or kept briefly in running seawater tanks in the laboratory at the Marine Biological Laboratory (Woods Hole, MA). Some of the *Mnemiopsis* were spawned in the laboratory to obtain 2–4-day cydippid larvae for light microscopy. *Bolinopsis infundibulum* (Müller, 1776) and *Pleurobrachia bachei* Agassiz, 1860, were collected at Friday Harbor, Washington, and used for electron microscopy (Tamm and Tamm, 1988).

Dissections

Specimens of *Mnemiopsis* or *Pleurobrachia* were temporarily pinned in a Sylgard 184-lined fingerbowl or petri dish of seawater placed on a transmitted light stage of a stereo microscope to first measure animal size. The aboral end of each animal, containing the statocyst region, was then cut off with dissecting scissors, trimmed with iridectomy scissors, and placed—aboral pole up—on a slide for aboral views of the statolith. For lateral views of the statolith in the sagittal or tentacular plane, 1–2-mm thick slices of the aboral ends of larger animals were cut parallel to either plane with dissecting and iridectomy scissors.

Light microscopy

Whole larvae or dissected tissue pieces of *Mnemiopsis* were individually transferred with wide-mouth pipets into a well of seawater on a microscope slide rimmed with petroleum jelly. Tissue pieces were positioned in the desired orientation, then coverslipped and immobilized by gentle compression. Slides were observed with a Zeiss DIC (differential interference contrast) microscope (16× or 40× objectives) and imaged with a Zeiss ZVS-3C75DE digital camera connected to a Panasonic AG-7355 VCR and QSI model VFF-6030 video frame/field counter allowing still frame/field playback (Tamm, 2012a, b). As in previous work, audio tracks of observations and identifications were recorded to accompany video images for playback analysis (Tamm, 2012a, b).

Analysis

Before dissection, an animal's size was determined by measuring body length (including lobes) along the aboral-oral axis. For animals less than 2.5-cm long, the measurements were made to the nearest 1 mm (in rare cases of an estimated range of ±1 mm, the average value to the nearest 0.5 mm was used). For larger animals, the measurements were made to the nearest 0.5 cm (in rare cases of a range of ±0.5 cm, the average value to the nearest 0.25 cm was used). For measurements of relative statolith size, selected video fields of aboral or lateral views were traced from enlarged images on a video monitor using matte acetate. The major (*a*), minor (*b*), and depth (*c*) axes of statoliths were measured from tracings to the nearest millimeter, and halved to obtain radii (semi-axes) for volume calculations. Still-field images for comparisons and figure production were printed on Sony UPC-1020 paper with a Sony UP-1200 video printer (Tamm, 2012a, b).

Results

Body plan and symmetry

Ctenophores display bilateral symmetry around their major longitudinal axis with the mouth at one pole (oral) and the apical sensory organ containing the statocyst at the other end (aboral). Two mutually perpendicular planes of symmetry run along the oral-aboral axis: the sagittal plane in which the flattened stomodaeum lies, and the tentacular plane passing through the two tentacle pouches (Fig. 1) (Tamm, 2014a, b).

Lobate ctenophores such as *Mnemiopsis* are somewhat compressed in the tentacular plane and expanded in the sagittal plane, with two oral lobes on either side of the

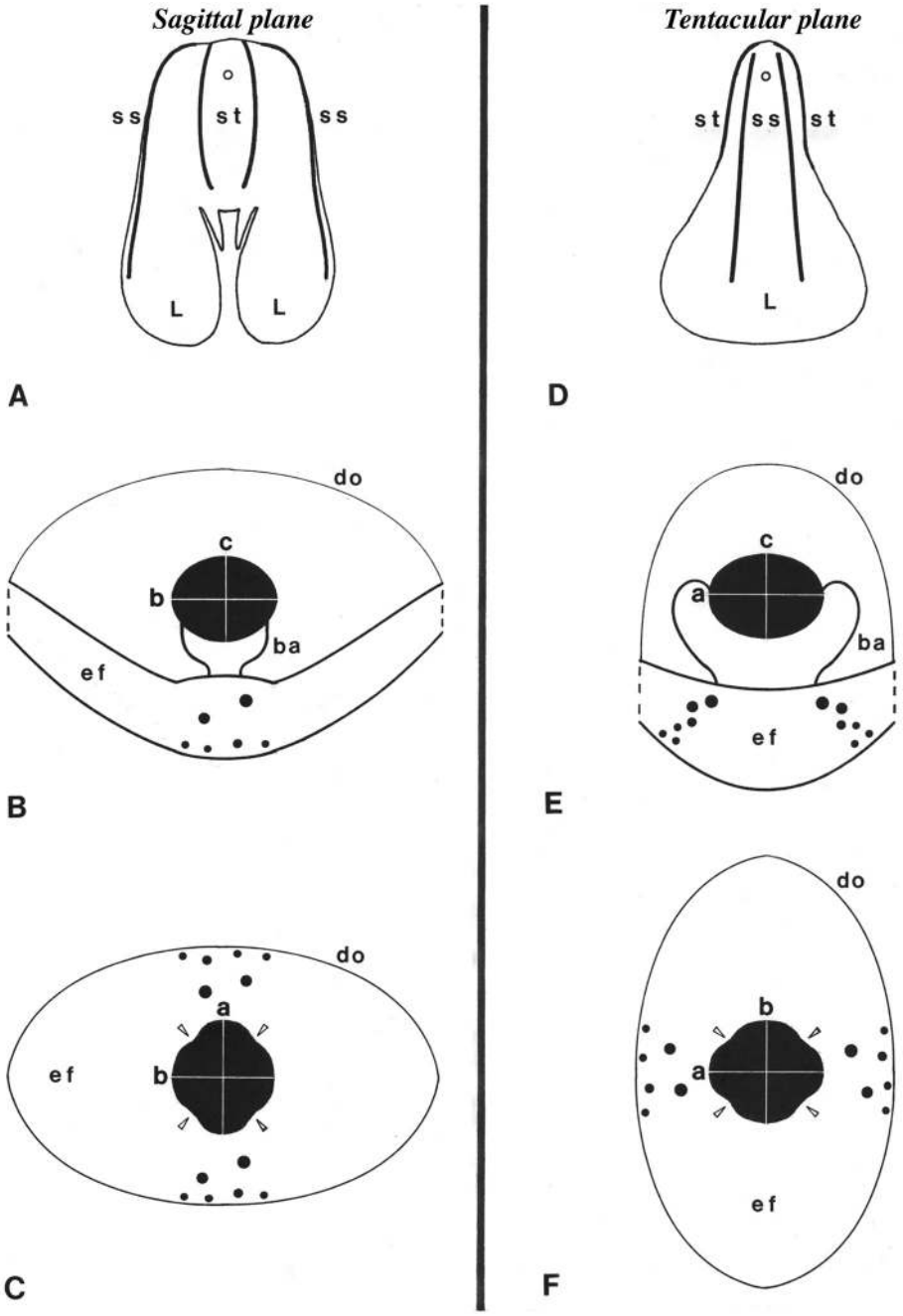

Figure 1. Diagram of a whole *Mnemiopsis*, and higher magnification of its statolith, as viewed in the sagittal plane (left column: A, B, C) and in the tentacular plane (right column: D, E, F). (A, D) Side views of an animal: its body is expanded in the sagittal plane (A) and compressed in the tentacular plane (D). The statocyst is located in the small open circle near the aboral end (upward). Two rounded lobes (L) and auricles project from either side of the mouth at the oral end (downward). The pair of tiny tentacles is not shown. The longer subsagittal comb rows (ss) and the shorter subtentacular comb rows (st) are represented by heavy black lines. (B, E) Side views of the statocyst in the sagittal (B) and tentacular (E) plane. Note the *a*, *b*, and *c* axes of the statolith (black) and the different spacing of the balancers (ba) in the two planes. Developing stages of lithocytes in the epithelial floor (ef) are shown by filled circles of different sizes. do, dome cilia. (C, F) Aboral views of the statocyst with the sagittal plane horizontal in (C) and the tentacular plane horizontal in (F). The four balancers (open triangles) are seen from their distal curved ends near the four notches in the statolith (black), whose major (*a*) and minor (*b*) axes are indicated. Comparing the location of the developing lithocytes (filled circles) with corresponding side views (B, E) enables a spatial reconstruction. The longer axis of the oval epithelial floor (ef) and base of the dome (do) is parallel to the sagittal plane (C) but perpendicular to the tentacular plane (F).

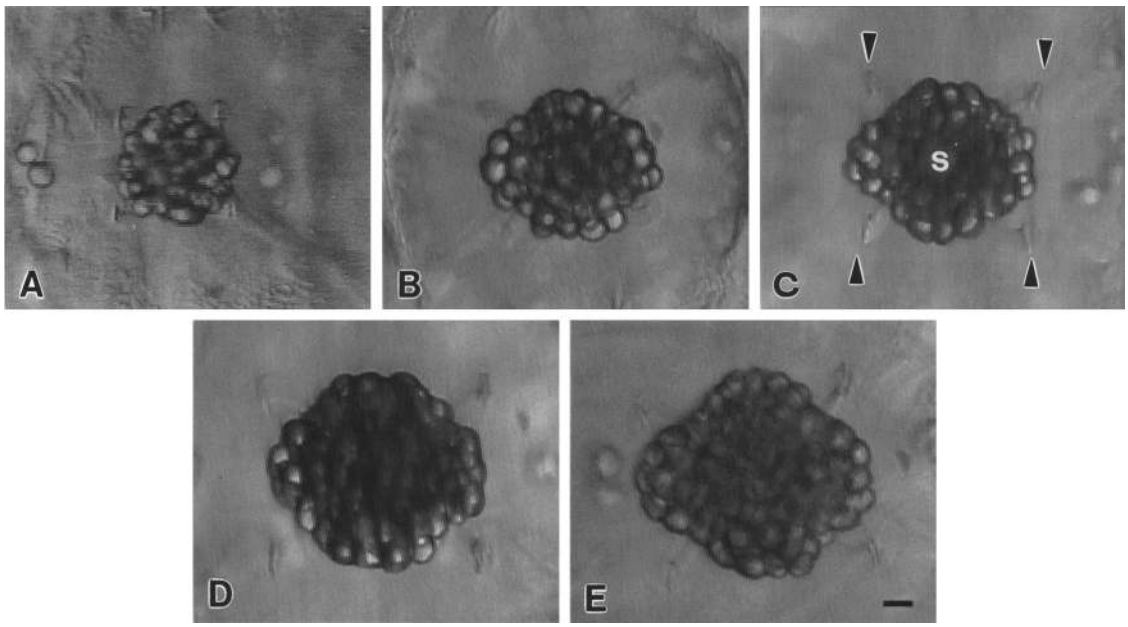

Figure 2. Aboral differential interference contrast views of statoliths containing multiple refractile lithocytes in animals of increasing body lengths: 4.5 mm (A), 9 mm (B), 2.5 cm (C), 4 cm (D), 5.5 cm (E). The images are oriented with the tentacular axis horizontal, but the left-right directions are arbitrary. The curved distal ends of the four balancers (arrowheads in C only) are in the notches of the statolith (s) at 45° to the tentacular and sagittal planes. The major *a*-axis of the superellipsoidal statolith runs horizontally parallel to the tentacular plane. The minor *b*-axis runs vertically, parallel to the sagittal plane. Note that the lithocyte size is similar in statoliths of all sizes. Scale bar, 10 μm.

mouth, which is surrounded by four ciliated auricles (Fig. 1A, D). The four subsagittal comb rows bordering the sagittal plane are longer than the four subtentacular rows along the tentacular plane (Fig. 1A, D).

Statolith shape, orientation, and size

A surprising finding was that the statolith of *Mnemiopsis* is not a spherical mass of lithocytes as generally supposed (Hyman, 1940; Horridge, 1971; Barnes, 1980; Tamm, 1982; Pearse *et al.,* 1987; Brusca and Brusca, 1990; Tamm and Tamm, 2002). Aboral views as well as lateral views (Figs. 1, 2, 3, 9) reveal that the statolith has a superellipsoidal shape—that is, a three-dimensional analog of a superellipse, a closed curve that is midway between an ellipse and a rectangle (Gardner, 1965). In many images the statolith resembles a superegg, a special case of a superellipsoid with blunt ends (Gardner, 1965).

The major *a* axis of the statolith is parallel to the tentacular plane, and the minor *b* axis is parallel to the sagittal plane (Fig. 1). Four clefts, or notches, at 45° to the tentacular and sagittal planes mark the locations and insertions of the four balancers. The superellipsoidal shape and orientation of the statolith correspond to the arrangement of the four balancer bases, which arise at the vertices of a rectangle with a length/width ratio of about 3:1, with the longer sides oriented parallel to the tentacular plane (Tamm and Tamm, 2002). As a result, two opposing pairs of closely set balancers are spaced widely apart along the tentacular plane (Fig. 1B, C, E, F) (Tamm, 1982, 2014a; Tamm and Tamm, 2002). The longer *a* axis of the statolith and wider spacing of the balancer pairs is thus orthogonal to the expanded sagittal plane of the somewhat flattened body of *Mnemiopsis* (Fig. 1). In addition, the thickened epithelial floor of the apical organ is not circular in area as previously illustrated (Hyman, 1940; Horridge, 1971; Barnes, 1980; Pearse *et al.,* 1987; Brusca and Brusca, 1990), but has an oval or superelliptical shape with its long axis parallel to the sagittal plane (Fig. 1C, F) (Tamm, 1982). The oval epithelial floor is humped along its short axis, which runs along the tentacular plane (Fig. 1B).

To investigate statolith size as a function of animal size, the major (*a*) and minor (*b*) axes of the statolith were measured in a plane normal to the aboral-oral axis. The depth of the statolith (*c*-axis) along the aboral-oral axis was not visible in these aboral views (Fig. 1C, F). However, the product of the major and minor axes (*ab*) is proportional to the sectional elliptical area through the center of the statolith in a medial plane normal to the aboral-oral axis. Since neither the volume nor the mass of the statolith could be measured, and since the true superellipsoidal shape with four corner notches could not be factored in, the sectional

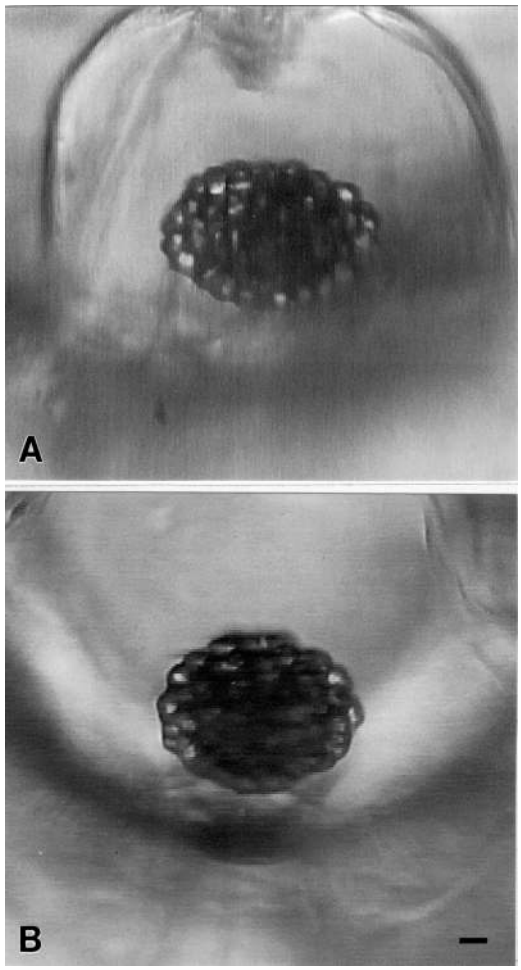

Figure 3. Lateral views of the statolith shape in thick tissue slices viewed parallel to each of the two body planes. Aboral direction is toward the top. The epithelial floor, balancers, and dome cilia are mostly out of focus due to the thickness of the preparations. (A) View in the tentacular plane from a 6–cm animal. The major *a*-axis runs horizontally, and the *c*-axis (depth) runs vertically through the center of the statolith. The superellipsoidal shape is seen from the side. (B) View in the sagittal plane from a 5-cm animal. The minor *b*-axis runs horizontally, and the *c*-axis runs vertically through the center of the statolith. The superellipsoidal statolith is seen from one end. Note that the opposing dome cilia walls are closer together in the tentacular plane (A) than in the sagittal plane (B), due to the hemi-ovoidal shape of the dome (see Fig. 1). Scale bar, 10 μm.

elliptical area (*ab*) was used as a convenient measure for comparing relative sizes of statoliths.

Statoliths of 2–4-day cydippid larvae do not yet have a superellipsoidal shape but a more irregular shape due to the large size of individual lithocytes relative to their small number at this stage (Fig. 4). Nevertheless, they can be used to estimate statolith size.

Figure 5 shows the relative sizes of statoliths in animals ranging in body lengths from about 0.5 mm (early cydippid larvae) to 7 cm (largest adults collected). Statolith size increases with animal size, and the rate of statolith growth is highest in younger stages, but the rate gradually decreases

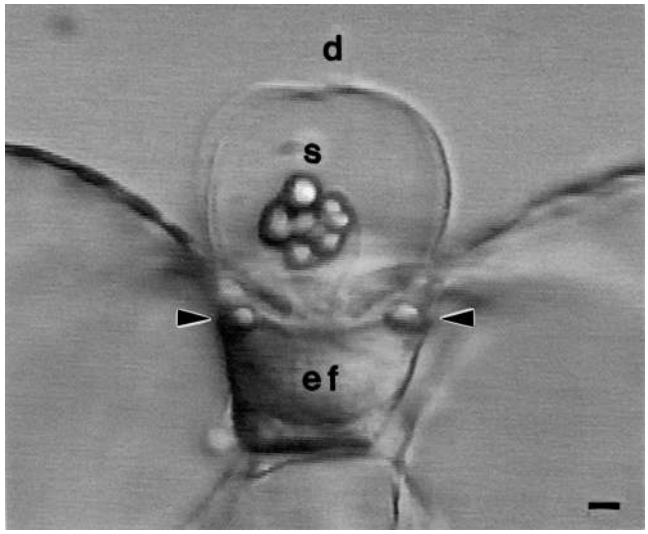

Figure 4. Apical organ (statocyst) of a 2-day *Mnemiopsis* cydippid larva viewed from the side in the tentacular plane by differential interference contrast optics. The thickened concave epithelial floor (ef) contains one lithocyte on either side (arrowheads). A statolith with seven visible lithocytes is supported by the balancers arising from the floor; one of the balancers is faintly seen on the right. Transparent dome cilia (d) enclose the statocyst cavity and do not appear motile at this stage. Scale bar, 10 μm.

as the animals become larger. Aboral images of the shape and size of statoliths in selected animals of increasing body size are illustrated in Figure 2. It is apparent that the size of individual lithocytes remains similar as their number increases in larger statoliths.

Statolith major/minor axis ratio (a/b) versus animal size

To determine whether the geometric proportions or Cartesian coordinates of the statolith, as viewed aborally,

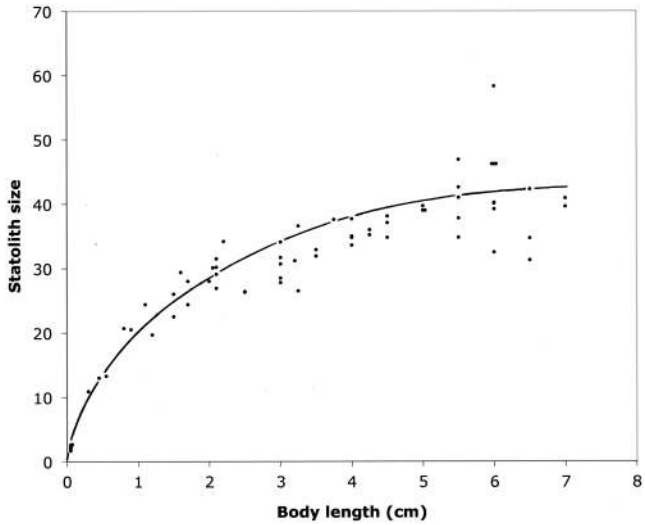

Figure 5. Relative statolith size (see text) as a function of body length in 68 animals. Statolith size increases with animal size, starting at a high growth rate in the earliest stages and declining in larger animals.

change with increasing body size, the ratio of the major to minor axes (*a*/*b*) was plotted as a function of body length (not shown). The *a*/*b* ratios showed wide scatter from 1.00 to 1.26 independent of ctenophore size. The mean of *a*/*b* ratios for all body sizes is 1.12 ± 0.07 ($n = 59$). The small standard deviation indicates little or no trend from a horizontal line with increasing body size (confirmed by a linear regression analysis), suggesting that the relative proportions of the statolith do not change significantly as the statolith enlarges with body size (Figs. 2, 5).

Number of lithocytes in the adult statolith

The refractile lithocytes are roughly spheroidal with a diameter of about 10 μm and a calculated cellular volume of about 525 μm^3 in both larvae and adults. The membrane-bound calcareous concretion fills most of the cell, and lithocytes are tightly packed together in the statolith (Tamm, 1982). In compressed larvae with spread, dissociated lithocytes, counts of the number of lithocytes per statolith gave means and standard deviations, as follows: 8 ± 1 lithocytes in 2-day larvae ($n = 21$), 9 ± 1 lithocytes in 3-day larvae ($n = 10$), and 11 ± 2 lithocytes in 4-day larvae ($n = 25$).

In 5- to 6.5-cm adults, lateral views of statoliths in tissue slices (Fig. 3) gave a mean *c*-axis radius in the tentacular plane of 28 ± 1.3 μm ($n = 3$), and a mean *c*-axis radius in the sagittal plane of 31 ± 2.6 μm ($n = 7$), or an average of about 30 μm for both lateral orientations. Corresponding measurements of the *a* axis in tentacular plane slices and the *b* axis in sagittal plane slices resulted in a mean *a*/*c* ratio of 1.4, and a mean *b*/*c* ratio of 1.2.

The number of lithocytes in statoliths of 6-cm adult *Mnemiopsis* was estimated by treating statolith shape as an ellipsoid and ignoring the clefts for the balancers. The mean *a* and *b* axis radii as viewed aborally for this ctenophore size class ($n = 8$) are 43 μm and 40 μm, respectively. Using a *c*-axis of 30 μm, the statolith volume is about 217,000 μm^3, and therefore contains about 400 lithocytes.

Lithocyte development

Lithocytes were found to develop at specific locations in the thickened, single-layered epithelial floor of the statocyst cavity (Fig. 1). Developing lithocytes are recognizable by their refractile concretions of various sizes, although cell boundaries are not discernible (Figs. 4, 6). Lithocytes arise on opposite sides of the epithelial floor along the tentacular plane, that is, at two sites bilateral to the sagittal plane (Figs. 1, 4, 6). The earliest stages appear as single small refractile granules or clusters of granules at the lower edge (basal lamina) of the concave epithelial floor (Fig. 6C). More apically, the inclusions appear fused together into single concretions that become progressively larger toward the apical surface of the epithelium (Figs. 1, 6). These stages of lithocyte development are found in the epithelial floor of all *Mnemiopsis* specimens examined, from early cydippid larvae to the largest adults (see below).

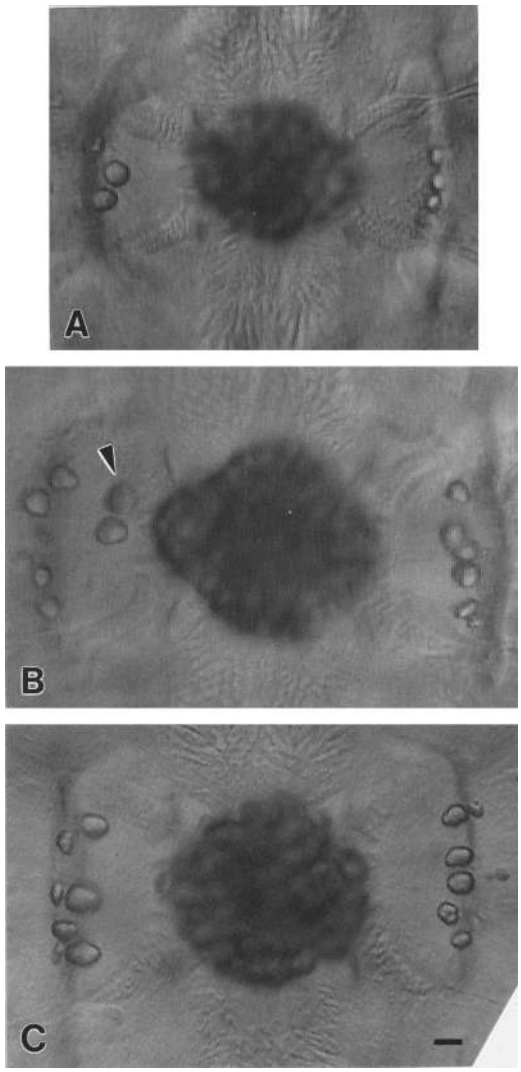

Figure 6. Aboral views of lithocyte development in the epithelial floor on opposite sides of the tentacular plane, which runs left-right. Earlier stages of differentiation of refractile lithocytes are smaller and located deeper and further laterally in the floor. Later stages are larger and closer to the balancers (their distal ends near the notches of the statolith are above the focal level). (A) A 9-mm animal with three developing lithocytes on each side of the floor. Four pairs of ciliated grooves are evident, resembling a cross-hatched X emanating from the central statolith. (B) A 5.5-cm animal with five developing lithocytes in the left side, and six lithocytes in the right side of the floor. Arrowhead indicates a freshly budded lithocyte which video records showed was jiggling on the base of the upper left balancer. The adjacent lithocyte in the floor, midway between the left pair of balancers, has not yet been released. (C) A 6.5-cm animal with seven developing lithocytes in the left side and six in the right side of the floor. Note smaller refractile granules or clusters of granules near the basal lamina at opposite edges of the floor. Scale bar, 10 μm. Panel 6B is the same preparation shown in Panel 2E, but the focus here is on the epithelial floor.

Figure 7. Transmission electron micrograph of a longitudinal thin section through the statocyst of a 4-day *Bolinopsis infundibulum* cydippid larva. Three adherent lithocytes (Li) plus a grazing section of a fourth one are visible in the statolith. Each lithocyte contains a large membrane-bound vacuole (v) which appears empty, surrounded by a peripheral nucleus (n) and cytoplasm. The vacuole (v) in a developing lithocyte in the epithelial floor contains concentric layers of electron-dense crystals and a small hole (see text). Dome cilia (d) arise from the edges of the floor. Scale bar, 1 μm.

In transmission electron micrographs of developing lithocytes in the epithelial floor of 4-day cydippid larvae of *Bolinopsis*, a related lobate ctenophore similar to *Mnemiopsis*, the intracellular vacuoles contain a peripheral layered shell of short, electron-dense needles and sometimes small irregular holes in the section (Fig. 7). This is in contrast to the uniformly empty appearance of the large vacuole in lithocytes of the small statolith at this stage (Fig. 7); in both cases the nucleus and cytoplasmic organelles are confined to the periphery (comparative electron micrographs of *Mnemiopsis* statoliths are not available). In adult statoliths of *Bolinopsis* and *Pleurobrachia*, the hard concretion filling the vacuole is displaced during sectioning, leaving a large hole, but not if tissue is treated with EGTA or EDTA during fixation (Tamm, 1982). Lithocytes in the statoliths of 4-day cydippid larvae of *Bolinopsis* thus resemble those in adults treated with calcium chelators. This may be due to a lower concentration of calcium salt in lithocytes of younger stages.

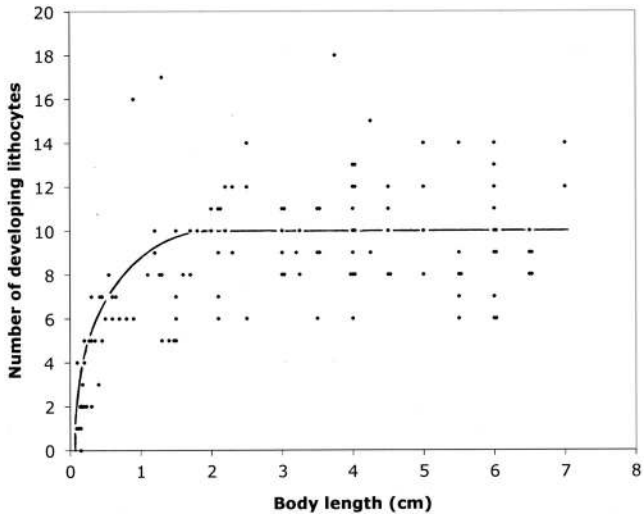

Figure 8. Total number of developing lithocytes at all stages in both sides of the epithelial floor in 127 animals of different sizes. The rate of increase of differentiating lithocytes is highest in the youngest animals and slows to reach a plateau range of 8–12 lithocytes with wide scatter in larger animals. Data from body lengths of 2- to 7-cm are fitted by a linear regression with no slope and a Y-intercept of 10 lithocytes.

Number of developing lithocytes in the epithelial floor

The number of developing lithocytes on opposite sides of the epithelial floor is usually similar in a given individual of *Mnemiopsis* (Fig. 6). Figure 8 shows the total number of developing lithocytes in animals of different sizes. Early cydippid larvae have on average two developing lithocytes (Fig. 4), and the number of developing lithocytes increases rapidly with animal size up to 1–2 cm, where the rate slows. In larger animals the number of developing lithocytes shows wide scatter at all body sizes, but within a uniform range of 8–12 lithocytes (Fig. 8). A linear regression of the data for body sizes from 2 to 7 cm gives a Y intercept of 10 lithocytes and an essentially horizontal line (Fig. 8). Lithocytes are therefore produced continually throughout the life of *Mnemiopsis*, and at a fairly similar rate in animals larger than 2-cm long.

Transport of budded lithocytes into the statolith

After lithocytes reach the apical surface of the floor, they were observed to bud off from the epithelium midway between the closely spaced bases of a pair of balancers along the tentacular plane. Aboral observations of statocysts in *Mnemiopsis* of various sizes show no consistent spatial pattern of release of lithocytes with respect to individual balancers. Liberation of lithocytes seems to occur infrequently and apparently randomly in animals of all ages, and probably depends on the distribution of developmental stages on opposite sides of the epithelial floor.

It was recently discovered in *Mnemiopsis* that liberated

lithocytes attach to the base of an adjacent balancer and then move distally up the surface of the balancer to the tip, where they join other lithocytes in the statolith (Noda, 2013). During this transport the attached lithocyte jiggles at the frequency of beating of the balancer it is riding on (Figs. 6B, 9), but its gliding movement is independent of balancer beating (Noda, 2013; this report). Lithocyte transport is driven by a type of ciliary surface motility and is believed to be powered by anterograde kinesin motors (Noda, 2013).

Lithocytes usually travel on the outer surface of a balancer and follow the curved distal end to its insertion at a notch of the statolith (Fig. 9). New lithocytes are therefore added exclusively at the four corner clefts where the balancers enter the statolith. Subsequent locations and possible re-arrangements of lithocytes within the aggregate, as well as their lifetime and eventual fate, have not yet been determined. Some lithocytes within a statolith make specialized adherent junctions with the distal ends of balancer cilia, thereby ensuring firm attachment of the statolith to the balancers (Tamm, 1982).

Motility of dome cilia

The statocyst cavity is enclosed by a transparent dome (veil, cupola) of rows of long, closely packed cilia (Fig. 10), which arise around the border of the thickened epithelial floor (Figs. 1, 7). Since the floor is not circular but oval, the dome is not hemispherical as previously assumed, but hemiovoidal (Figs. 1, 3, 11).

The dome cilia have previously been described as nonmotile (Tamm, 1982). However, new observations reveal that the dome cilia display coordinated movements. Flagellar-like waves start at the ciliary bases and propagate distally to the ciliary tips roofing over the statocyst (Fig. 11). The mean velocity of the waves is 6.1 $\pm$ 1.7 μm/s (n = 10), and the frequency is about 8 waves/min. Wave total displacement (twice the amplitude) is 10–15 μm, which diminishes distally. Viewed aborally, dome ciliary waves sometimes progress synchronously to the top of the dome, like an undulating curtain over the statocyst (Fig. 11). In other preparations, different sectors around the base of the dome initiate waves (or fail to) at different times. The slow, low-amplitude propagated waves of dome cilia are observed in both young and adult *Mnemiopsis*, but not in very early cydippid stages (Fig. 4) nor in some adult preparations. The function of dome ciliary motility may be related to the newly discovered process of statolith formation by lithocyte transport up the balancers (see Discussion).

Pleurobrachia *statocyst*

Pleurobrachia, a member of the order Cydippida, is more radially symmetric than lobate ctenophores and has nearly equal sagittal and tentacular axes with all comb rows being of similar length (Tamm, 2014a). Aboral and lateral views

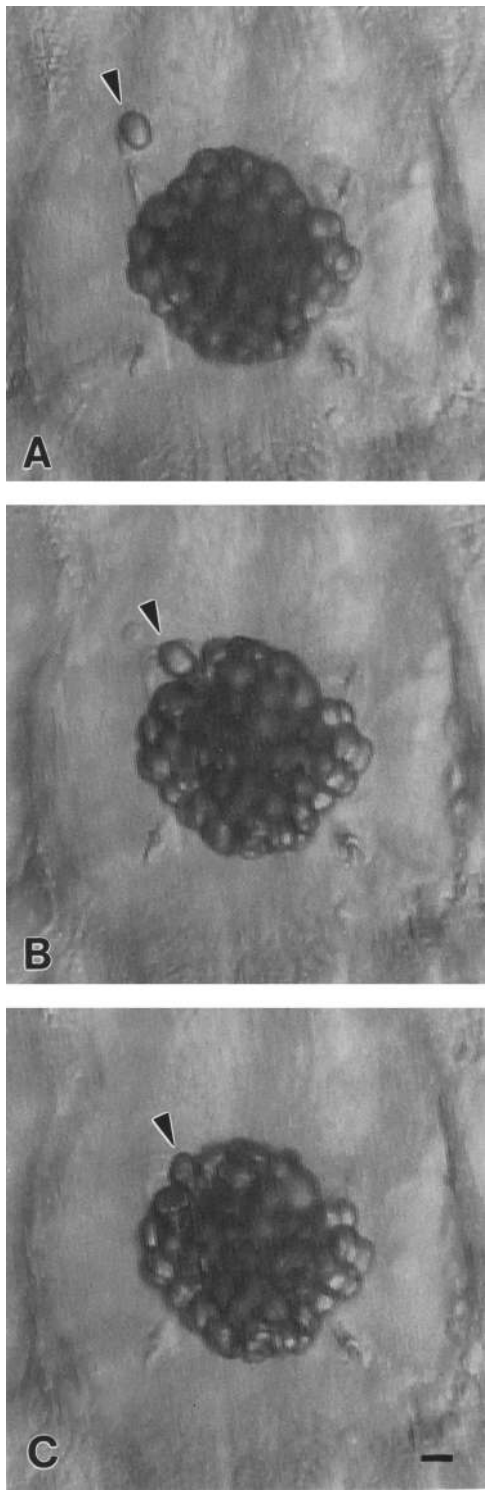

Figure 9. Aboral view of a lithocyte (arrowhead) gliding into the statolith on the upper left balancer in a 2.1-cm animal. The tentacular plane is left-right, and the distal ends of the four balancers are visible at the four notches of the statolith. (A) The lithocyte moves up the outside of the curved distal region of the balancer, jiggling with the beating of the balancer. (B) The lithocyte approaches the notch where the balancer inserts into the statolith. (C) The lithocyte joins the other lithocytes in the statolith. Scale bar, 10 μm.

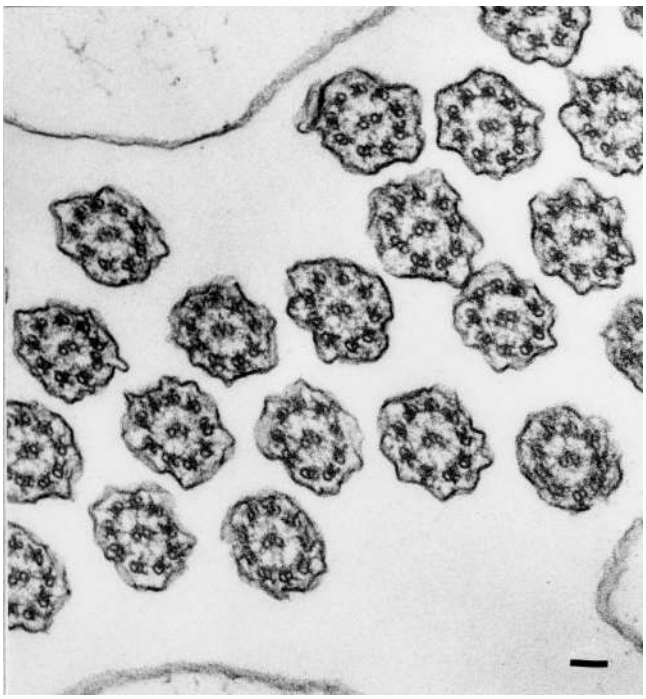

Figure 10. Transmission electron micrograph of a cross-section through the dome wall of a *Pleurobrachia pileus* adult. The rows of regularly spaced cilia in the dome wall run from lower left to upper right. The central pair of microtubules are oriented parallel to the wall at right angles to the plane of propagated bending waves. Scale bar, 100 nm.

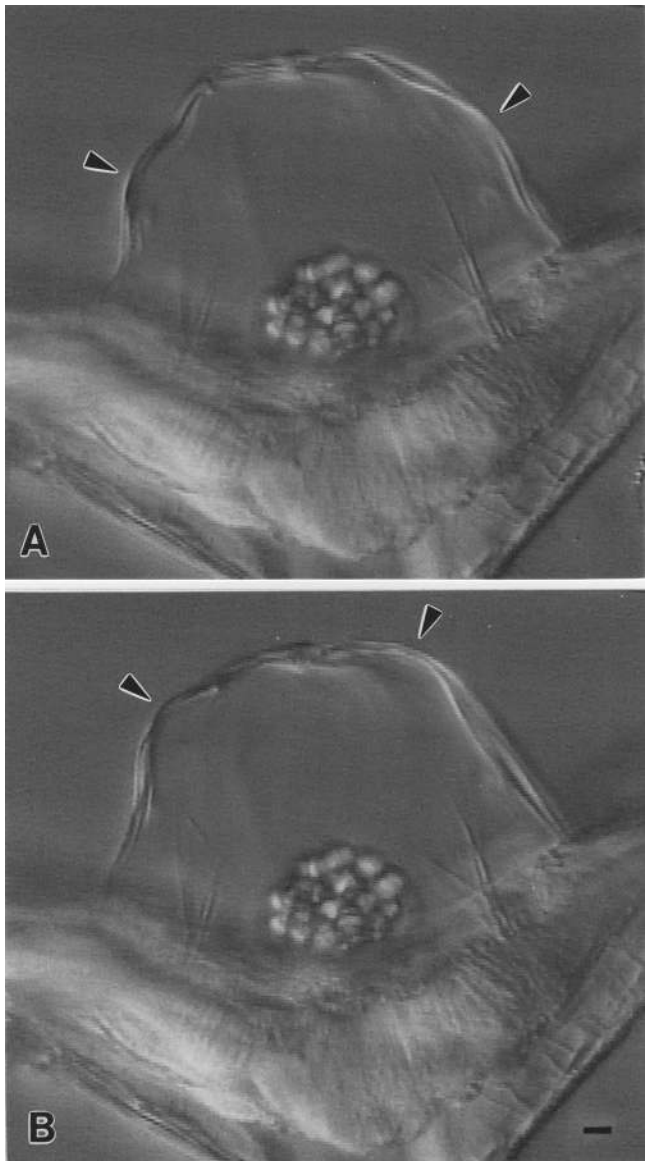

Figure 11. A pair of sequential lateral views in the sagittal plane of dome cilia motility in a 7-mm individual of *Mnemiopsis*. The focal plane lies about midway through the dome, and includes the concave epithelial floor and the statolith. (A, B) Waves on either side of the dome (arrowheads) start at the base of the cilia and propagate distally to the roof at similar speeds. Note the hemi-ovoidal profile of the dome in this plane (see Fig. 3). Groups of bristle-like projections of unknown nature are evident on either side of the statolith (see Tamm, 2014a). Scale bar, 10 μm.

of dissected statocyst regions of adult *Pleurobrachia* of various sizes showed that its statolith also has a superellipsoidal shape with the major *a* axis oriented parallel to the tentacular plane, and with four corner notches marking the locations of the four rectangularly arranged balancers. As found in *Mnemiopsis*, lithocytes develop in the oval epithelial floor on opposite sides along the tentacular plane. Budded lithocytes are transported up balancers into the statolith, as in *Mnemiopsis* (Noda, 2013). Motility of the dome cilia in *Pleurobrachia* is generally similar to that in *Mnemiopsis.*

Thus, the shape, orientation, and body plane symmetry of the statocyst in *Pleurobrachia* is the same as in *Mnemiopsis*, regardless of the differences in relative length of the sagittal and tentacular axes (and body shape) between adult animals of these orders.

Discussion

The novel findings of this report are (1) the superellipsoidal instead of spherical shape of the ctenophore statolith, (2) orientation of the major axis of the statolith along the tentacular plane, (3) distinct migration paths of developing lithocytes through the epithelial floor to reach the bases of the balancers, (4) continual production of lithocytes and enlargement of the statolith throughout the life of *Mnemiopsis*, and (5) wave-like motility of the dome cilia enclosing the statocyst cavity. The similarity in findings between the lobate *Mnemiopsis* and the cydippid *Pleurobrachia*, members of two different orders of ctenophores, suggests that these features of the statocyst may be common in the phylum.

We confirm transport of newly budded lithocytes up the balancers to build the statolith in *Mnemiopsis* (Noda, 2013)

and extend this finding to *Pleurobrachia*. In both ctenophores, this route of lithocyte delivery results in four clefts at the corners of the statolith for the supporting balancers. The significance of these findings is discussed below.

Unique features of the ctenophore statocyst

The statocyst of ctenophores is unique among invertebrates in not using nerves or muscles to mediate orientation with respect to gravity (Tamm, 1982, 2014a, b). Geotaxis is performed directly by a hierarchy of mechanically coordinated ciliary organelles: balancers, ciliated grooves, and locomotory comb plates. In response to the deflection of the balancers by the statolith, balancer beat frequency is modulated by calcium-dependent mechanotransduction (Lowe, 1997), and neural input only overrides the geotactic response or switches its sign (Lowe, 1997; Tamm, 1982, 2014a, b).

The superellipsoidal shape of the statolith is another unique feature of the ctenophore statocyst. Superellipses and their three-dimensional analogs, the superellipsoid and superegg, were discovered by Piet Hein (Gardner, 1965). Nature, as it turns out, has not only invented the wheel (Tamm, 2008), but also the superellipse!

The superellipsoidal shape of the ctenophore statolith and the orientation of its major axis along the tentacular plane is clearly the result of both the rectangular (instead of square) placement of the four balancers on the epithelial floor, and the mode of addition of freshly budded lithocytes to the ends of the statolith by transport up the balancers themselves. The asymmetric ratio of the rectangular spacing of the four balancers, which is about 3:1 in the tentacular *versus* sagittal planes, is significantly greater than the major/minor axis ratio of 1.12 for the statolith in the tentacular *versus* sagittal planes. The architecture and orientation of the multicellular statolith of ctenophores thus appears to be determined mainly by the geometry of its balancer cilia scaffold, which supplies new lithocytes so that the statolith grows only at its two ends.

An important functional question is whether these asymmetries of statolith morphology and orientation with respect to the sagittal and tentacular body planes affect the function of the statocyst during geotaxis. Previous quantitation of beat frequency responses of the balancers and comb rows to graded angular tilting of a ctenophore did not take into account (or alter) the body plane in which the animal was tilted (Tamm, 1980, 1982). Future experiments should reveal whether the new anatomical findings described here have behavioral consequences during geotaxis.

The relative size of the statolith increases nonlinearly with animal size (body length). The rate of statolith growth is highest in the youngest stages and gradually decreases with increasing body size (Fig. 5). Whether the statolith continues to grow in animals larger than 7 cm is not known, but seems likely. Based on volumetric calculations, a statolith of a large adult of *Mnemiopsis* contains about 400 lithocytes.

Chun (1880) first observed that statolith concretions (he thought they were solely extracellular products) arise in the epithelial floor along the tentacular plane on opposite sides of the statocyst cavity. We confirmed this location for developing lithocytes, and found that visible differentiation of lithocytes begins with the secretion of small refractile inclusions near the basal lamina at opposing ends of the epithelial floor along the tentacular plane (Fig. 6).

Progressive stages of developing lithocytes follow a diagonal path toward the apical surface (Fig. 1E), parallel to the long axes of the tall epithelial cells in the concave floor. Their translocation through the epithelium may be driven by active motility of the developing lithocytes themselves or of the neighboring cells, or both. Lithocytes are budded off midway between the closely set bases of each pair of balancers along the tentacular plane. This convenient proximity to their ciliary delivery route into the statolith is due to the place of origin of lithocytes in the epithelial floor and their path to the apical surface. Which member of a balancer pair is used to transport a newly released lithocyte could depend on a chance encounter with the closest balancer base, but evidence is lacking.

The total number of developing lithocytes (on both sides of the epithelial floor) in an animal was found to increase rapidly in younger animals, and then reach a plateau range of 8–12 lithocytes in ctenophores larger than about 2 cm. Comparing the kinetics of lithocyte formation (Fig. 8) to that of statolith growth (Fig. 5) as a function of animal size, both processes start at maximal rates and increase rapidly in younger stages. But the rate of lithocyte formation attains its largest values at a body length of about 2 cm, whereas the statolith itself is still increasing significantly in size at this stage.

The relation between lithocyte supply and demand is complicated by the absence of time or age data to correlate with our morphological measurements. Furthermore, statoliths, being perched atop the balancers, are metabolically isolated from the rest of the ctenophore. Their lithocytes may have a finite "shelf life" and may turn over and be replaced during the lifetime of the animals. If so, continual production of lithocytes in the epithelial floor may be required to provide not only for enlargement of the statolith, but for replacement of its lithocytes as well.

The finding that lithocytes are continually produced throughout adult life suggests the existence of two permanent populations of adult stem cells for lithocytes, localized basally at opposite sides of the epithelial floor along the tentacular plane. Injection of fluorescent lineage tracers (DiI) into identified blastomeres of *Mnemiopsis* embryos showed that lithocytes originate from oral micromeres of the E lineage and continue to produce new lithocytes in the

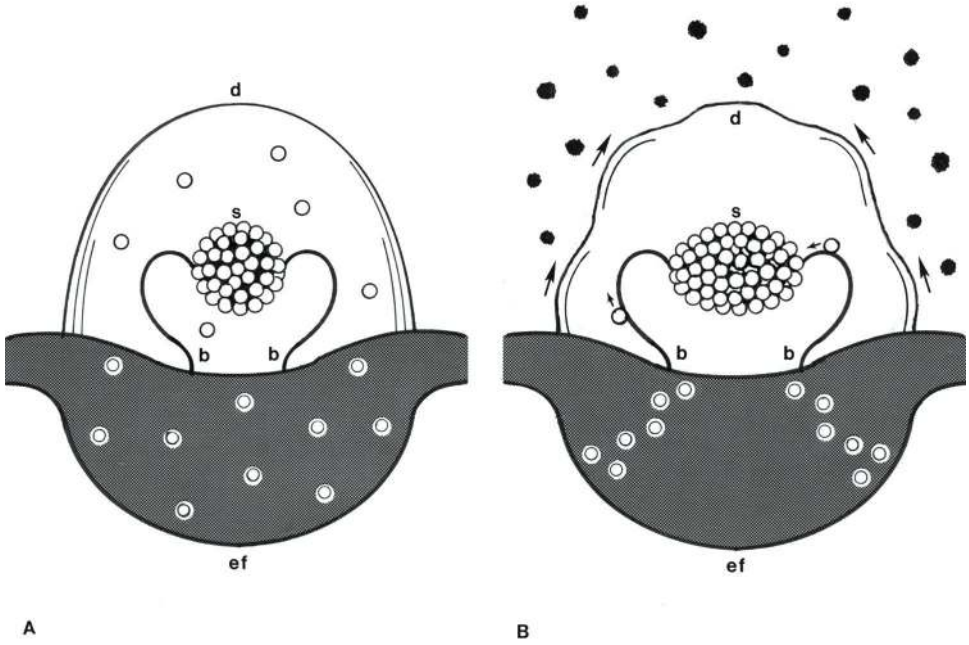

Figure 12. Old and new views of the ctenophore statocyst. Statocysts are viewed in the tentacular plane with the aboral direction upward. Only one balancer (b) of each pair is shown. Lithocytes are depicted as open circles in the statolith (s), under the dome (d), and in the epithelial floor (ef). Model (A) Lithocytes arise throughout the epithelial floor and bud off under a nonmotile ciliary dome, randomly colliding and adhering to the tips of equidistant balancers to form a spherical statolith. Model (B) Lithocytes arise exclusively from opposite sides of the epithelial floor along the tentacular plane, and bud off next to widely spaced balancer pairs on which they are transported distally (small arrows) to form a superellipsoidal statolith. Dome cilia propagate waves distally (large arrows) which deflect and prevent foreign particles (black bodies) from entering the statocyst cavity and being transported up the balancers into a dysfunctional statolith.

epithelial floor throughout adult life (Martindale and Henry, 1999). In this regard, Alié *et al.* (2011) used *Piwi* and *Vasa* as germline and stem cell marker genes and found spatially restricted somatic stem cell pools for cells of comb plates, tentacles, and polar fields—but not for lithocytes in the statocyst floor—in *Pleurobrachia*.

Possible role of dome cilia in statolith formation

Previously, it was thought that lithocytes arise and bud off generally from the epithelial floor of the statocyst, and that the enclosing ciliary dome prevents their escape into the surrounding seawater, thereby facilitating their aggregation and attachment to the tips of the balancers (Tamm, 1982) (Fig. 12A).

The new findings reported here and by Noda (2013) suggest that the dome cilia do not act as a container to keep available lithocytes inside, but may do just the opposite: keep foreign, potentially disruptive objects out. In support of this idea, lithocytes are rarely seen circulating freely under the dome, from the time they bud off the floor to being transported up the balancers into the statolith. Experiments on the mechanism of transport showed that not only lithocytes but also inert polystyrene microspheres of similar size are transported distally to balancer tips (Noda, 2013). The ciliary surface motility thus cannot distinguish real lithocytes from foreign objects of similar size.

The dome cilia may therefore screen out external particles that could be mistaken for lithocytes, preventing them from contacting balancers and being included in a functionally defective statolith. The peristaltic, distally propagated waves of the dome ciliary curtain may enhance this rejection mechanism by deflecting and clearing impinging objects away from the dome wall (Fig. 12B).

This model also accounts functionally for the cargo size dependence of direction of transport along balancers: 1-μm-diameter polystyrene beads, much smaller than lithocytes, undergo bidirectional saltatory transport along balancers, and usually do not reach the balancer tips (Noda, 2013). Such smaller foreign particles may slip through the motile dome screen, or even occur as breakdown products within the statocyst cavity itself.

However, the motility of dome cilia is not apparent in early larval stages and in some adults, and it has not been determined whether these individuals contain extraneous

particles under their non-waving domes. Other possible functions of dome cilia motility, such as hydrodynamic flow or feedback for statolith position and balancer deflection, or keeping adherent particles from obscuring light detection by photoreceptors in the epithelial floor, also suffer from the lack so far of consistent dome motility in all ctenophores examined, and the possible effects and reasons why. The function of the dome cilia remains an unsolved question in understanding the life of ctenophores.

In conclusion, this study shows how a combination of morphology, development, and physiology contributes to an understanding of the biological construction of a complex and elegant gravity receptor organ in an early (or the first) metazoan.

Acknowledgments

I thank Signhild Tamm and the MBL Central Microscopy Facility for transmission electron microscopy, Mark Terasaki for help and support, Naoki Noda for his work on lithocyte transport, and Susan Banks for expert assistance in scanning figures.

Literature Cited

Alié, A., L. Leclère, M. Jager, C. Dayraud, P. Chang, H. Le Guyader, E. Quéinnec, and M. Manuel. 2011. Somatic stem cells express *Piwi* and *Vasa* genes in an adult ctenophore: ancient association of "germline genes" with stemness. *Dev. Biol.* **350:** 183–197.

Aronova, M. 1974. Electron microscopic observations on the aboral organ of ctenophores. *Z. Mikrosk. Anat. Forsch.* **88:** 401–412.

Barnes, R. D. 1980. *Invertebrate Zoology.* 4th ed. Saunders College, Philadelphia.

Brusca, R. C., and G. J. Brusca. 1990. *Invertebrates.* Sinauer, Sunderland, MA.

Budelmann, B.-U. 1988. Morphological diversity of equilibrium receptor systems in aquatic invertebrates. Pp. 757–782 in *Sensory Biology of Aquatic Animals,* J. Atema, R. R. Fay, A. N. Popper and W. N. Tavolga, eds. Springer-Verlag, New York.

Bullock, T. H., and G. A. Horridge. 1965. *Structure and Function in the Nervous Systems of Invertebrates,* Vols. I & II. Freeman, San Francisco.

Chun, C. 1880. Die Ctenophoren des Golfes von Neapel und der angrenzenden Meeres-Abschnitte. *Flora und Fauna des Golfes von Neapel,* Vol. 1. Engelmann, Leipzig.

Gardner, M. 1965. The "superellipse": a curve that lies between the ellipse and the rectangle. *Sci. Amer.* **213:** 222–236.

Hernandez-Nicaise, M.-L. 1991. Ctenophora. Pp. 359–418 in *Microscopic Anatomy of Invertebrates,* Vol. 2, *Placozoa, Porifera, Cnidaria, and Ctenophora,* F. W. Harrison and J. A. Estfall, eds. Wiley-Liss, New York.

Horridge, G. A. 1965. Relations between nerves and cilia in ctenophores. *Am. Zool.* **5:** 357–375.

Horridge, G. A. 1969. Statocysts of medusa and evolution of stereocilia. *Tissue Cell* **1:** 341–353.

Horridge, G. A. 1971. Primitive examples of gravity receptors and their evolution. Pp. 203–221 in *Gravity and the Organism,* S. A. Gordon and M. J. Cohen, eds. University of Chicago Press, Chicago.

Hyman, L. H. 1940. *The Invertebrates: Protozoa through Ctenophora.* McGraw-Hill, New York.

Krisch, B. 1973. Über das Apikalorgan (Statocyste) der Ctenophore *Pleurobrachia pileus. Z. Zellforsch.* **142:** 241–262.

Lowe, B. 1997. The role of calcium in deflection-induced excitation of motile mechanoresponsive balancer cilia in the ctenophore statocyst. *J. Exp. Biol.* **200:** 1593–1606.

Martindale, M. Q., and J. Q. Henry. 1999. Intracellular fate mapping in a basal metazoan, the ctenophore *Mnemiopsis leidyi,* reveals the origins of mesoderm and the existence of indeterminate cell lineages. *Dev. Biol.* **214:** 243–257.

Noda, N. 2013. Live cell moving on cilia: lithocyte movement on ciliary bundles during the statolith formation of ctenophore. American Society for Cell Biology Meeting. *Mol. Biol. Cell* **24:** #1980 (abstract).

Pang, K., and M. Q. Martindale. 2008. Comb jellies (Ctenophora): a model for basal metazoan evolution and development. *CSH Protoc.* doi:10.1101/pdb.emo106.

Pearse, V., J. Pearse, M. Buchsbaum, and R. Buchsbaum. 1987. *Living Invertebrates.* Blackwell Scientific, Palo Alto, CA.

Ryan, J. F., K. Pang, C. E. Schnitzler, A. D. Nguyen, R. T. Moreland, D. K. Simmons, B. J. Koch, W. R. Francis, P. Havlak, NISC Comparative Sequencing Program, S. A. Smith, *et al.* 2013. The genome of the ctenophore *Mnemiopsis leidyi* and its implications for cell type evolution. *Science* **342:** 1242592. DOI: 10.1126/science.1242592.

Samassa, P. 1892. Zur Histologie der Ctenophoren. *Arch. Mikrosk. Anat.* **40:** 157–243.

Tamm, S. L. 1980. Cilia and ctenophores. *Oceanus* **23:** 50–59.

Tamm, S. L. 1982. Ctenophora. Pp. 266–358 in *Electrical Conduction and Behaviour in 'Simple' Invertebrates,* G. A. B. Shelton, ed. Oxford University Press, Oxford.

Tamm, S. L. 2008. Unsolved motility looking for answer. *Cell Motil. Cytoskeleton.* **65:** 435–440.

Tamm, S. L. 2012a. Regeneration of ciliary comb plates in the ctenophore *Mnemiopsis leidyi.* I. Morphology. *J. Morphol.* **273:** 109–120.

Tamm, S. L. 2012b. Patterns of comb row development in young and adult stages of the ctenophores *Mnemiopsis leidyi* and *Pleurobrachia pileus. J. Morphol.* **273:** 1050–1063.

Tamm, S. L. 2014a. Cilia and the life of ctenophores. *Invertebr. Biol.* **133:** 1–46.

Tamm, S. L. 2014b. Ctenophores and termites—systems for motility. Pp. 147–171 in *Cilia and Flagella. Ciliates and Flagellates,* K. Hausmann and R. Radek, eds. Schweizerbart, Germany.

Tamm, S. L., and S. Tamm. 2002. Novel bridge of axon-like processes of epithelial cells in the aboral sense organ of ctenophores. *J. Morphol.* **254:** 99–120.

Tamm, S., and S. L. Tamm. 1988. Development of macrociliary cells in *Beroë.* I. Actin bundles and centriole migration. *J. Cell Sci.* **89:** 67–80.